EXPERIMENTAL AND THEORETICAL STUDIES OF THE PROPERTIES OF COHERENT SMITH-PURCELL RADIATION

F. Bakkali Taheri[a], I.V. Konoplev[a], G. Doucas[a], A. Reichold[a], R. Bartolini[a,b], N. Delerue[c], J. Barros[c], C. Clarke[d]

[a]JAI, Department of Physics, University of Oxford, Keble road, OX1 3RH, Oxford, UK
[b]also at Diamond Light Source Ltd., OX11 0QX, Oxfordshire, UK
[c]LAL, Univ. Paris-Sud, CNRS/IN2P3, Université Paris-Saclay, Orsay, France
[d]SLAC National Accelerator Laboratory, 2575 Sand Hill Road, Menlo Park, CA 94025, USA

Abstract

Recent advances in physics of particles accelerators and lasers have shifted dramatically the expectations of bunch length and capability to generate electron bunches with specific longitudinal profiles [1,2]. This has stimulated interest in analysis of spectrum of coherent radiation to enable the longitudinal bunch profile diagnostics at femtosecond-scale. Spectral analysis of coherent Smith-Purcell radiation (cSPr) is particularly relevant as it allows non-invasive and cost-effective monitoring of electron bunch profiles. In this paper, the recent results observed from the E203 experiment (FACET, SLAC) are presented. Consistency of the cSPr as diagnostic tool is discussed, as well as the properties of cSPr such as directionality and polarization.

INTRODUCTION

Smith-Purcell radiation occurs when a bunch of charged particles propagates in the vicinity of a periodic structure. In the far field region, the wavelength of the detected radiation varies with the angle θ, in accordance with the dispersion relation:

$$\lambda = \frac{\ell}{m}\left(\frac{1}{\beta} - \cos\theta\right) \qquad (1)$$

where l is the period of the grating along z (Fig.1), m is the order of radiation, β is the electron beam relative velocity with respect to the speed of light c, θ is the angle in xz plane (Fig.1) with $\theta=\pi/2$ corresponding to a normal direction toward the grating. Several mathematical models have been constructed in order to explain the radiation characteristics, and the most satisfying to date is the surface-current theory [2-4], which defines the theoretical framework of our analysis. The surface-current theory is constructed under the assumption that the radiation emitted by the grating, can be seen as the radiation of the surface current at the each facet while the surface current is induced by the electron bunch propagating in the vicinity of the grating.

THE E203 EXPERIMENT AT SLAC

The E203 experiment took place at SLAC from 2011 to 2015, and the design of its core apparatus has been described in [2-4]. The main components of the time profile monitor consist of a set of four metallic targets, three gratings and a blank.

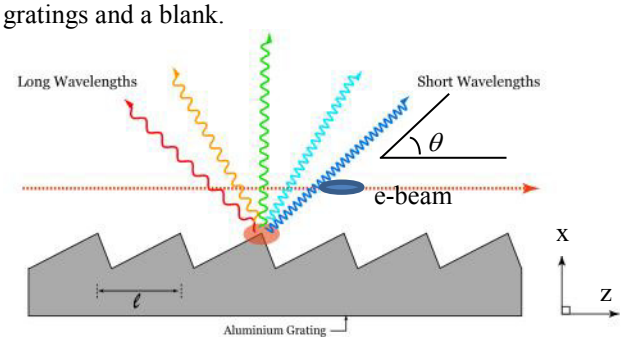

Figure 1: Schematic of electron beam propagating above the grating and excitation of Smith-Purcell radiation. Expression 1 is illustrated by showing the dependence of radiation wavelength on the observation angle.

For each grating, a filter is set up that selects the corresponding frequency bandwidth defined by (1). They are placed on a carrousel located in a vacuum chamber. The carousel rotates, permitting change of gratings to measure spectrum in different frequency ranges. The signal emitted from each grating is analysed after subtraction of the signal from blank target. This removes all non-cSPr contributions such as background (environmental) radiation, diffraction radiation from the grating edges, etc. The aim of the recent set of experiments was to study the directionality of the cSPR and its degree of polarization. Opportunity was also taken to check the consistency of cSPr as bunch length diagnostic tool.

The bunches had the following parameters: energy 20 GeV, number of electrons per bunch $1.8*10^{10}$ electrons, and a normalized emittance of 57 mm.mrad. The transverse dimensions (FWHM) were from 0.15 to 0.3 mm.

CSPR DIRECTIONALITY STUDY

In these studies, we measured the cSPr for each grating and blanc, through slits located at each port at 155 mm distance from the target. The slits were moving transversally across the ports (radius 10mm) from -10 to +10 mm positions by 0.5 mm step (0.18° angular step along the azimuthal angle ϕ) Fig.2. The measurements were carried

out at several beam-grating separations ranging from 2.24 mm to 8.25mm. We noticed that in many cases, cSPr exhibited a symmetrical structure with respect to $\phi=0^{\circ}$. In Fig.2, such dependences are illustrated for all the values angles ϕ°. One sees that all curves have a local minimum at $\phi=0^{\circ}$ and from each side of this local minimum, the azimuthal signal increases before decaying at larger ϕ. At 4° of each side, there is essentially no more cSPr signal.

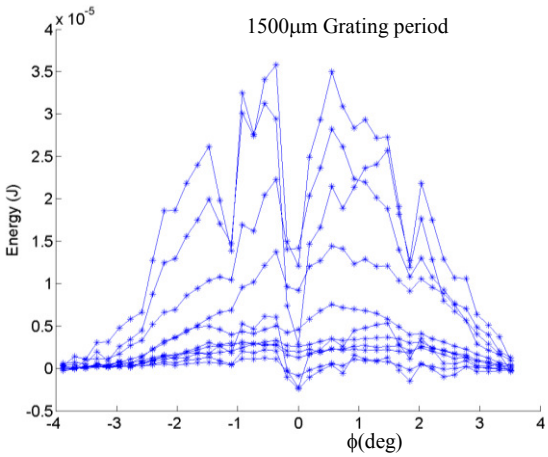

Figure 2: The dependences of the signal energy on the azimuthal angle ϕ observed for the set of angles $\theta\in(40^{\circ};140^{\circ})$ with step 10°.

Each point of the plot is the averaging of a fixed number of typically 100 measurements and has thus an associated error bar (standard deviation) which have been omitted for clarity on this plot, but they were re-introduced in the subsequent plots.

One of the objectives of the studies was to compare the experimental results with the semi-analytical predictions of the surface-current model. In Fig.3 such a comparison is shown. The blue curve is the theoretical prediction, while the two others are constructed from experimental data. In order to make an accurate comparison, we need to take into account two types of uncertainties: first, the standard deviation that arises from the bunch distribution at averaging. Then, we need to take into account the responsivity of a single detector for which only maximum and minimum values are well known. As a result, two extremal experimental curves define the region of validity of the data. The curves are plotted on the basis of the maximum and minimum responsivity of the detectors.

Fig. 3 shows two typical examples (at $\theta=60^{\circ}$ and $\theta=70^{\circ}$) and a good agreement between theoretical and experimental data can be clearly seen. The data observed for the 1500 micron grating located at 2.24 mm distance from beam. In both cases, the curves, predicted by the surface-current theory, fall between the maximum and minimum responsivity curves and comparable with the experimental data.

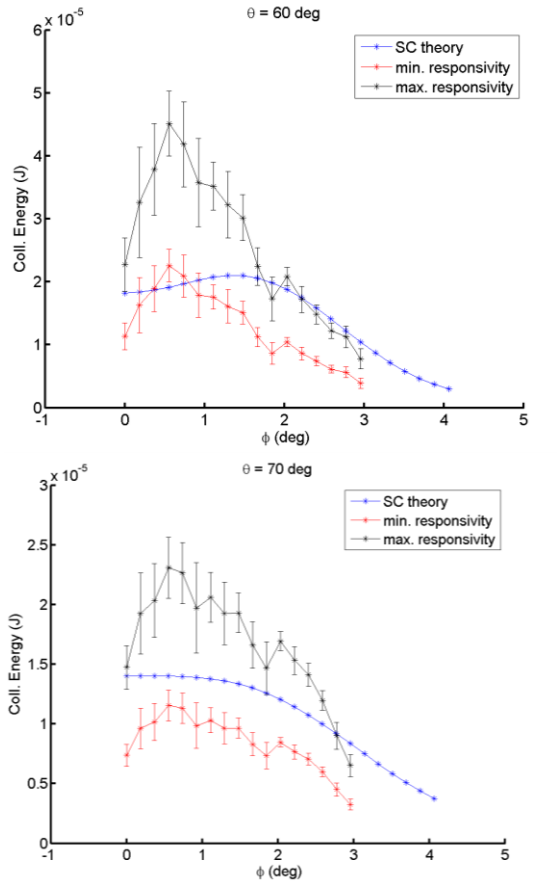

Figure 3: Comparison of the simulated ϕ-distribution with the experimental data for a 1500 microns period grating.

POLARIZATION

During the experiments, the polarization of the cSPr has also been studied for a fixed number of channels [1-3]. A polarizer was placed and two detectors were collecting, respectively, transmitted through (T), and reflected (R) at right angle radiation. As a result we will call these two polarization component respectively T and R. The measurements were taken for all gratings as well as the blank, at various distances of beam grating separation ranging from 1 mm to 4.5 mm. Fig. 4 shows an example of T and R measurements for the $\theta = 90^{\circ}$ and radiation generated by the 500 microns gratings, after background subtraction. Using this data it is possible to calculate the degree of polarization P:

$$\mathrm{P} = \frac{T-R}{T+R}$$

One of our most important results is the confirmation that, in the context of the E203, environmental and back ground radiations were unpolarised. Fig. 5 illustrates this showing that the degree of polarisation of the background is negligible i.e. comparable with zero and taking into account the associated uncertainties it can be ignored. For example at 1 mm, the measured degree of polarization was 0.065± 0.035, but at 1.5mm it drops to zero. One can compare the degree of polarization of cSPr signal ob-

ISBN 978-3-95450-147-2

tained after background subtraction with the degree of polarisation of the "pure" background. The degree of polarisation of the cSPr varies in the range from 0.55 to 0.85 (Fig.6) while maximum value of P=0.065 for the background. We observe a drop of degree of polarisation at small distances between beam and the grating. This can be partially explained due to large halo around the beam at FACET facilities which could introduce additional unpolarised transition and diffraction radiations. An increase of uncertainties at large beam-grating separations is due to the increase of relative errors, but the overall polarization plot has a reasonably flat response, as one should expect.

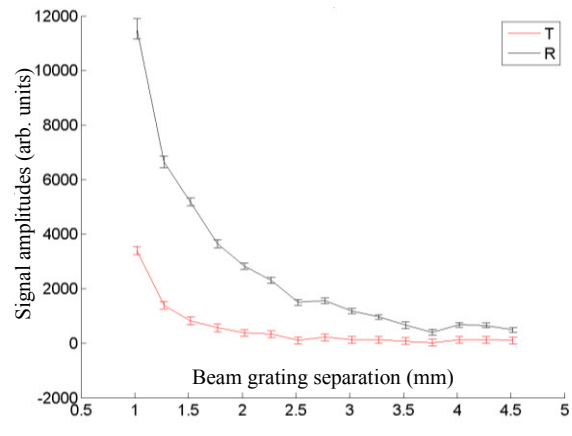

Figure 4: Experimental dependence of the two polarization components with the beam-grating separation.

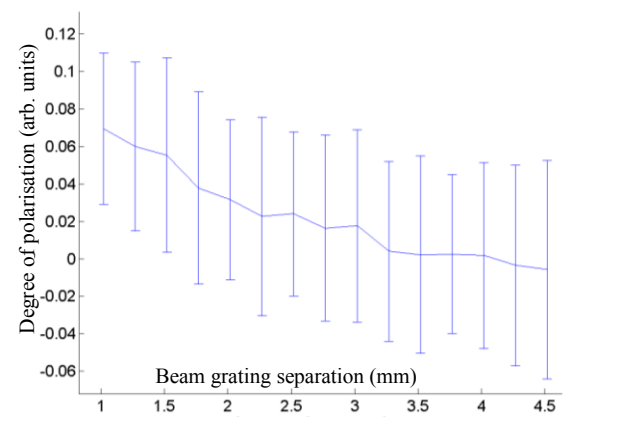

Figure 5: Degree of polarization from the background as measured at θ =90°.

CONCLUSION

In this work we presented results from the recent experiment at FACET, SLAC. An overview of the studies of the cSPr directionality i.e. radiation distribution along polar angle was presented, and shown to be in a good agreement with the surface-current model. A summary of polarization studies of both background radiation and cSPr were also shown data is analysed. The results are important for next step i.e. development of single shot cSPr bunch profile monitor. We discussed uncertainties presented during experiment and illustrated that a good agreement between semi-analytical and experimental data can be seen.

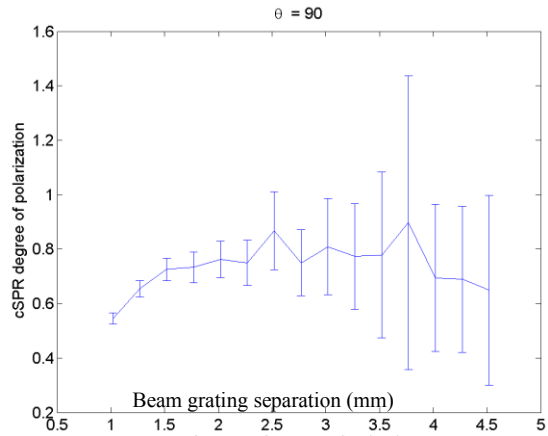

Figure 6: Degree of polarization of the cSPR signal as measured at θ=90° for the 500 micron period grating.

ACKNOWLEDGMENT

Mr. F. Bakkali Taheri would like to thank the STFC UK, for the support of this project. This work was performed [in part] under US Dept. of Energy Contract DE-AC02-7600515. Mr. N. Delerue would like to thank the French ANR for the support of this project (contract ANR-12-JS05-0003-01).

REFERENCES

[1] M. Litos, et al., Nature, 515, 92, 2014.

[2] C. G. R. Geddes, et al., Nature, 431, 538, 2004.

[3] G. Doucas, et al., Phys. Rev. STAB, 9, 092801, 2006.

[4] H. L. Andrews, et al., Phys. Rev. ST Accel. Beams 17, 052802, 2014.